Journal of the Arkansas Academy of Science

Volume 72 Article 8

2018

Wave Profile for Current Bearing Lightning Strokes

Baylee Landers
Arkansas Tech University, baylee.landers@yahoo.com

M Hemmati
Arkansas Tech University, mhemmati@atu.edu

Ali Alzhrani
Arkansas Tech University, aalzhrani@atu.edu

Recommended Citation

Landers, Baylee; Hemmati, M; and Alzhrani, Ali (2018) "Wave Profile for Current Bearing Lightning Strokes," *Journal of the Arkansas Academy of Science*: Vol. 72 , Article 8.
DOI: https://doi.org/10.54119/jaas.2018.7222
Available at: https://scholarworks.uark.edu/jaas/vol72/iss1/8

Wave Profile for Current Bearing Lightning Return Strokes

B. Landers[1], M. Hemmati[1]*, and A. Alzhrani[1]

[1]*Department of Physical Sciences, Arkansas Tech University, Russellville, Arkansas 72801, USA*

Correspondence: mhemmati@atu.edu

Running Title: Wave Profile for Current Bearing Lightning Return Strokes

Abstract

The propagation of breakdown waves in a gas, which is primarily driven by electron gas pressure, is described by a one-dimensional, steady-state, three-component (electrons, ions, and neutral particles) fluid model. This study will involve waves propagating in the opposite direction of the electric field force on electrons (anti-force waves—lightning return stroke) only. We consider the electron gas partial pressure to be much larger than that of the other species and the waves to have a shock front. Our set of equations consists of the equations of conservation of the flux of mass, momentum, and energy coupled with the Poisson's equation. The set of equations is referred to as the electron fluid dynamical equations.

For breakdown waves with a significant current behind the shock front, the set of electron fluid dynamical equations and also the boundary condition on electron temperature need to be modified. For a range of experimentally measured current values and a range of possible wave speeds, we will present the method of solution of the set of electron fluid dynamical equations and also the wave profile for electric field, electron velocity, electron temperature, and number density, as well as the ionization rate within the dynamical transition region of the wave.

Introduction

Electron shock waves are the propagating processes that convert an ion-less gas into a neutral plasma. A small amount of gas is ionized near the discharge electrode, and the resulting high-temperature electron gas expands rapidly, which yields an electron shock wave. Also, free electrons are accelerated by the electric field until they have enough energy to ionize the neutral gas through collisions. There are two types of breakdown waves: proforce waves and antiforce waves. Proforce waves are waves for which the electron velocity is in the same direction as the direction of the propagation of the wave. Antiforce waves are waves for which the electron velocity is in the opposite direction as the direction of the propagation of the wave; however, we assume the electron gas partial pressure to be large enough to provide the required force for the propagation of the wave. Antiforce waves are the lightning return strokes, which are the subject of our investigation. The wave has two distinct regions: A thin dynamical transition region, referred to as the sheath region of the wave, directly following the shock front, and a relatively thicker thermal region (referred to as the quasi-neutral region). In the thin dynamical transition region, electric field, starting from its maximum value at the shock front, reduces to zero at the end of the sheath, and the electrons, starting from an initial speed at the shock front slow down to speeds comparable to the speed of the ions and heavy particles. In the thermal region, electrons cool down to approximately room temperature by further ionization of the heavy particles.

Model

To develop the model for current-bearing antiforce waves, one must start with the basic equations for proforce waves. These equations, developed by Shelton and Fowler (1968) and completed by Fowler et al. (1984), are a one-dimensional fluid-dynamical model. The set of equations is comprised of the equations for conservation of mass, momentum, and energy along with Maxwell's equations, which reduces to Poisson's equation only and are given as

$$\frac{d(nv)}{dx} = n\beta \tag{1}$$

$$\frac{d}{dx}\left[mnv(v-V) + nkT_e\right] = -enE - Kmn(v-V) \tag{2}$$

$$\frac{d}{dx}[nmv(v-V)^2 + nkT_e(5v-2V) + 2envφ + \varepsilon_0 VE^2 -$$

$$\frac{5nk^2T_e}{mk}\frac{dT_e}{dx}] = -(\frac{m}{M})[3nkKT_e + nmK(v-V)^2] \quad (3)$$

$$\frac{dE}{dx} = \frac{en}{\varepsilon_0}(\frac{v}{V}-1) \quad (4)$$

Variables *E, x, β, K, V, M, E_o,* and *φ* represent the electric field, position within the wave, ionization frequency, elastic collision frequency, wave velocity, neutral particle mass, electric field at the wave front, and ionization potential respectively. The remaining variables, *e, T_e, n, v,* and *m,* are the charge, temperature, concentration, velocity, and mass for electrons.

Next, a set of dimensionless variables developed by Fowler *et al.* (1984) are used to reduce Equations (1-4) to their non-dimensional form. These variables are

$$\eta = \frac{E}{E_o}, \nu = (\frac{2e\phi}{\varepsilon_o E_o^2})n, \psi = \frac{v}{V}, \theta = \frac{T_e k}{2e\phi}, \xi = \frac{eE_o x}{mV^2},$$
$$\alpha = \frac{2e\phi}{mV^2}, \kappa = \frac{mV}{eE_o}K, \mu = \frac{\beta}{K}, \omega = \frac{2m}{M},$$

Here, *ν, ψ,* and *θ* are the dimensionless electron concentration, velocity and temperature, while *μ, η,* and ξ are the dimensionless ionization rate, electric field, and position inside the wave. Equations (1-4) in their new, non-dimensional form are

$$\frac{d(\nu\psi)}{d\xi} = \kappa\mu\nu, \quad (5)$$

$$\frac{d}{d\xi}[\nu\psi(\psi-1)+\alpha\nu\theta] = -\nu\eta - \kappa\nu(\psi-1), \quad (6)$$

$$\frac{d}{d\xi}[\nu\psi(\psi-1)^2 + \alpha\nu\theta(5\psi-2) + \alpha\nu\psi + \alpha\eta^2 - \frac{5\alpha^2\nu\theta}{\kappa}\frac{d\theta}{d\xi}] = -\omega\kappa\nu[3\alpha\theta + (\psi-1)^2], \quad (7)$$

$$\frac{d\eta}{d\xi} = \frac{\nu}{\alpha}(\psi-1). \quad (8)$$

To change these equations for proforce waves such that they apply to the antiforce case, one must define a set of variables similar to the ones used above. These dimensionless variables, introduced by Hemmati (1999), are as follows:

$$\eta = \frac{E}{E_o}, \nu = (\frac{2e\phi}{\varepsilon_o E_o^2})n, \psi = \frac{v}{V}, \theta = \frac{T_e k}{2e\phi}, \xi = -\frac{eE_o x}{mV^2},$$
$$\alpha = \frac{2e\phi}{mV^2}, \kappa = -\frac{mV}{eE_o}K, \mu = \frac{\beta}{K}, \omega = \frac{2m}{M}.$$

where again *ν, ψ,* and *θ* are the dimensionless electron concentration, velocity and temperature, while *μ, η,* and ξ are the dimensionless ionization rate, electric field, and position inside the wave.

By implementing this second set of variables into the original, one-dimensional proforce equations, Equations (1-4), one reduces them to a dimensionless form while also converting them for use in the antiforce case. The non-dimensional equations describing antiforce waves are

$$\frac{d}{d\xi}[\nu\psi] = \kappa\mu\nu, \quad (9)$$

$$\frac{d}{d\xi}[\nu\psi(\psi-1)+\alpha\nu\theta] = \nu\eta - \kappa\nu(\psi-1), \quad (10)$$

$$\frac{d}{d\xi}[\nu\psi(\psi-1)^2 + \alpha\nu\theta(5\psi-2) + \alpha\nu\psi - \frac{5\alpha^2\nu\theta}{\kappa}\frac{d\theta}{d\xi} + \alpha\eta^2] = -\omega\kappa\nu[3\alpha\theta + (\psi-1)^2], \quad (11)$$

$$\frac{d\eta}{d\xi} = -\frac{\nu}{\alpha}(\psi-1). \quad (12)$$

For current bearing antiforce waves, Hemmati *et al.* (2011) gives the current as

$$I_1 = eN_iV_i - enν$$

where N_i and V_i are the ion number density and velocity behind the wave front respectively.

Solving this for N_i and then substituting it into the Poisson's equation gives the following.

$$\frac{dE}{dx} = \frac{e}{\varepsilon_0}(\frac{I_1}{eV} + \frac{n\nu}{V} - n)$$

Substituting in the dimensionless variables for antiforce waves as well as introducing dimensionless current, given by

$$\iota = \frac{I_1}{\varepsilon_0 K E_0}$$

reduces the Poisson's equation to the following.

$$\frac{d\eta}{d\xi} = \kappa\iota - \frac{\nu}{\alpha}(\psi-1).$$

https://scholarworks.uark.edu/jaas/vol72/iss1/8
DOI: https://doi.org/10.54119/jaas.2018.7222

Solving this for $v(\psi-1)$ and substituting it into the equation for conservation of energy gives the full set of non-dimensional equations for current bearing antiforce waves, which are

$$\frac{d}{d\xi}[v\psi] = \kappa\mu\nu, \tag{13}$$

$$\frac{d}{d\xi}[v\psi(\psi-1)+\alpha v\theta] = v\eta - \kappa v(\psi-1), \tag{14}$$

$$\frac{d}{d\xi}[v\psi(\psi-1)^2+\alpha v\theta(5\psi-2)+\alpha v\psi-\frac{5\alpha^2 v\theta}{\kappa}\frac{d\theta}{d\xi} + \alpha\eta^2] = 2\eta\kappa\iota\alpha-\omega\kappa\nu[3\alpha\theta+(\psi-1)^2], \tag{15}$$

$$\frac{d\eta}{d\xi} = \kappa\iota - \frac{\nu}{\alpha}(\psi-1). \tag{16}$$

Results and Discussion

Since antiforce waves are observed in nature as lightning return strokes, values measured from real lightning strokes can be used to assess the fluid model. For the average speeds of lightning return strokes, Idone *et al*. (1987) have reported values in the range of $0.9\text{x}10^8$ to $1.6\text{x}10^8$ m/s. Mach and Rust (1992) reported an average of $0.8\text{x}10^8$ to $1.7\text{x}10^8$ m/s, while Nakano *et al.* (1987) measured a wide range of speeds from $0.3\text{x}10^8$ to $2\text{x}10^8$ m/s. In our analysis of antiforce waves, we have been able to find solutions to the model for speeds as low as $2\text{x}10^6$ m/s.

For the currents measured in lighting return strokes, averages ranging from less than 10kA to more than 40kA were reported for different regions of the US by Orville and Huffines (1999). In Japan, meanwhile, currents up to 340kA were reported from direct measurements by Goto and Narita (1995).

As for the temperatures reported, Jurenka and Barreto (1985) estimate the neutral air in a lightning channel to be at a range of 4000 to 8000K. For the temperature of the electrons inside the wave, they estimate a value of around 20,000K.

Electron number density was also reported by Jurenka and Barreto (1985). In their paper they give a range of 10^{10} to 10^{12} el./cm^3 and greater.

We have integrated equations (13-16) through the sheath region using a trial and error method. First, values are selected for dimensionless wave speed, α, and current, ι. We then adjusted values for electron velocity, ψ_1, electron number density, ν_1, at the wave front and the wave constant, κ, and integrated through the sheath region and repeated this process until the solutions met the excepted physical conditions at the trailing edge of the wave ($\eta_2 \to 0$ as $\psi_2 \to 1$). For a relatively large speed, α=0.001, we have been able to integrate our set of electron fluid dynamical equations for a set of six different dimensionless current values—ι=0.5, 0.7, 1, 2, 5, and 10. α=0.001 represents an actual wave speed value of $9.37\text{x}10^7$ m/s.

The set of initial conditions which resulted in successful integration of the set of equations is as follows:

α=0.001, ι=0.5, κ=0.144, ψ_1=0.51721, ν_1=0.1750
α=0.001, ι=0.7, κ=0.144, ψ_1=0.5142, ν_1=0.167
α=0.001, ι=1, κ=1.44, ψ_1=0.514, ν_1=0.1816
α=0.001, ι=2, κ=1.44, ψ_1=0.5093, ν_1=0.1857
α=0.001, ι=5, κ=0.144, ψ_1=0.4855, ν_1=0.1953
α=0.001, ι=10, κ=0.144, ψ_1=0.442, ν_1=0.199

Figure 1 represents dimensionless electric field, η, as a function of dimensionless electron velocity, ψ, within the sheath region of the wave. Note that the graphs for all values of dimensionless currents, except for ι=10, meet the expected conditions at the end of the sheath region. The largest value of current that gave a proper solution was ι=7.

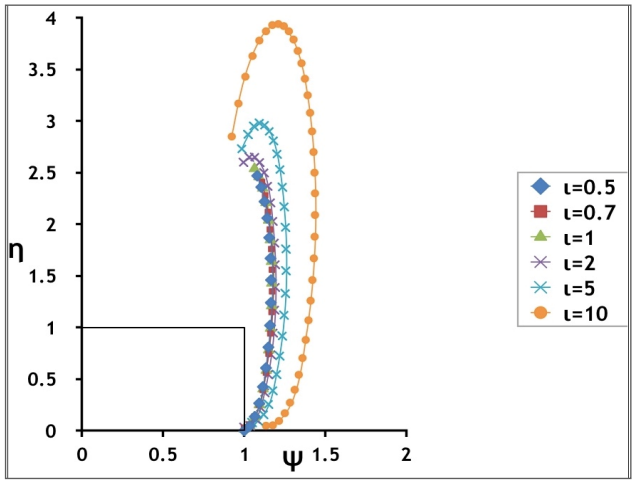

Figure 1. Electric field, η, as a function of electron velocity, ψ, within the sheath region of current bearing antiforce waves for a wave speed value of α=.001 and for current values of 0.5, 0.7, 1, 2, 5, and 10.

Figure 2 represents dimensionless electron velocity, ψ, as a function of dimensionless position, ξ, within the sheath region of the wave. The graphs show that as current increases, sheath thickness increases.

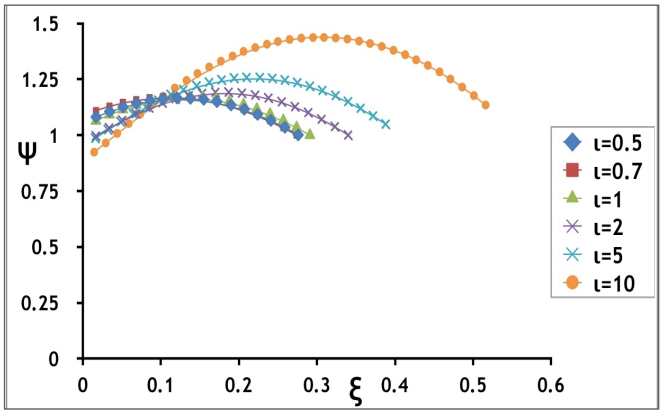

Figure 2. Electron velocity, ψ, as a function of position, ξ, within the sheath region of the current bearing antiforce waves for a wave speed value of α=0.001 and for current values of 0.5, 0.7, 1, 2, 5, and 10.

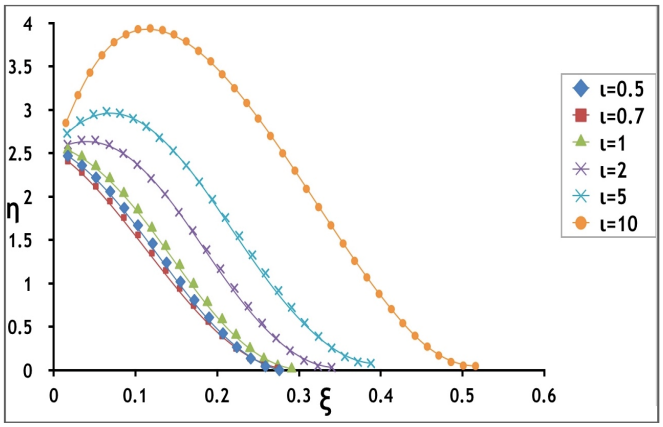

Figure 3. Electric field, η, as a function of position, ξ, within the sheath region of the current bearing antiforce waves for a wave speed value of α=0.001 and for current values of 0.5, 0.7, 1, 2, 5, and 10.

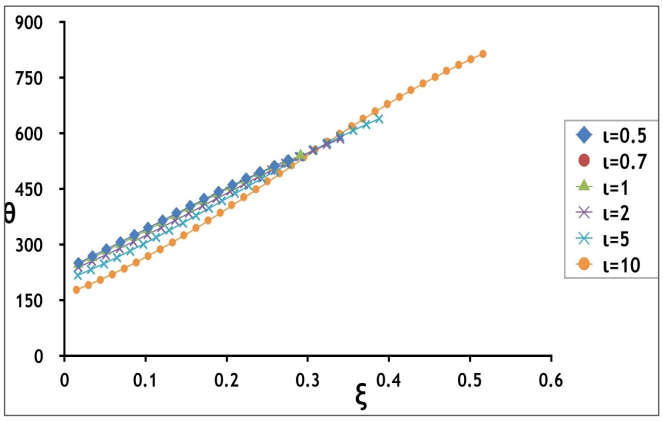

Figure 4. Electron temperature, θ, as a function of position, ξ, within the sheath region of the current bearing antiforce waves for a wave speed value of α=0.001 and for current values of 0.5, 0.7, 1, 2, 5, and 10.

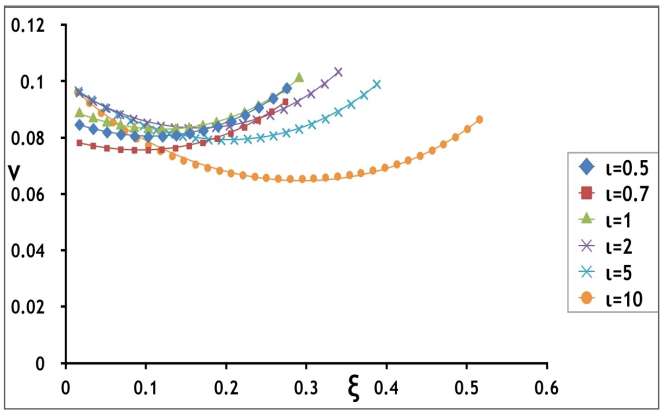

Figure 5. Electron number density, ν, as a function of position, ξ, within the sheath region of the current bearing antiforce waves for a wave speed value of α=0.001 and for current values of 0.5, 0.7, 1, 2, 5, and 10

Figure 3 represents dimensionless electric field, η, as a function of dimensionless position, ξ, within the sheath region of the wave. It is seen that, for all values of ι, the expected conditions at the trailing edge of the wave are met, that is at the end of the sheath region η goes to zero.

Figure 4 represents dimensionless electron temperature, θ, as a function of dimensionless position, ξ, within the sheath region of the wave. As one traverses through the sheath region of the wave, the electron temperatures increases.

Figure 5 represents dimensionless electron number density, ν, as a function of dimensionless position, ξ, within the sheath region of the wave. For all ι values, ν initially decreases and then increases again to almost the initial values.

As we increase the wave speed, it can support higher currents. ι = 1 approximately represents an actual current value of 10kA, and α = 0.001 represents an actual wave speed value of 9.37×10^7 m/s. For α=0.001, we have been able to solve our set of electron fluid dynamical equations for dimensionless current as high as ι = 7. Rakov (2000) reports a speed range of 0.3×10^8 to 2×10^8 m/s and a peak current of up to 300kA. Therefore, we should be able to solve the equations for much higher currents than the 5 to 35kA generally reported. For antiforce waves, Rakov (2000) gives the lower end of the speed range as 0.3×10^8 m/s.

We have been able to integrate our set of equations for considerably lower wave speeds as well. This means that slower antiforce waves than reported are possible to observe.

In addition to the six dimensionless current values

https://scholarworks.uark.edu/jaas/vol72/iss1/8
DOI: https://doi.org/10.54119/jaas.2018.7222

for α=0.001, we have been able to integrate our set of equations for dimensionless wave speed values of α=1, which is equivalent to an actual wave speed as low as $2.96x10^6$ m/s and a dimensionless current value as high as ι = 0.25, as well as for α=0.1, which represents an actual wave speed of $9.37x10^6$ m/s, and a dimensionless current as high as ι = 1.

Figure 6 represents the dimensionless electric field, η, as a function of dimensionless electron velocity, ψ, within the sheath region of the wave. Both graphs meet the expected conditions at the end of the sheath region.

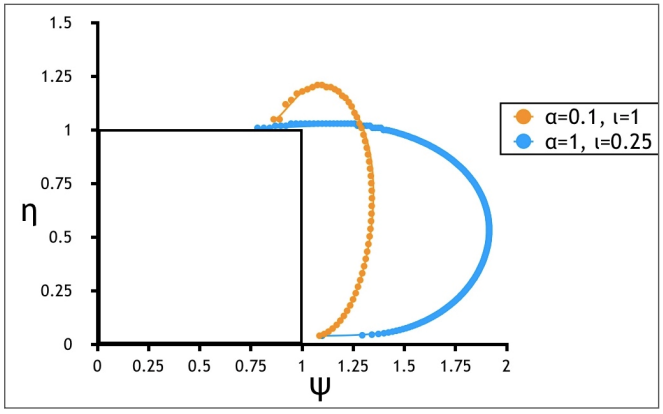

Figure 6. Electric field, η, as a function of electron velocity, ψ, within the sheath region of current bearing antiforce waves for wave speed values of α=0.1 and 1 and for current values of ι= 1 and 0.25 respectively.

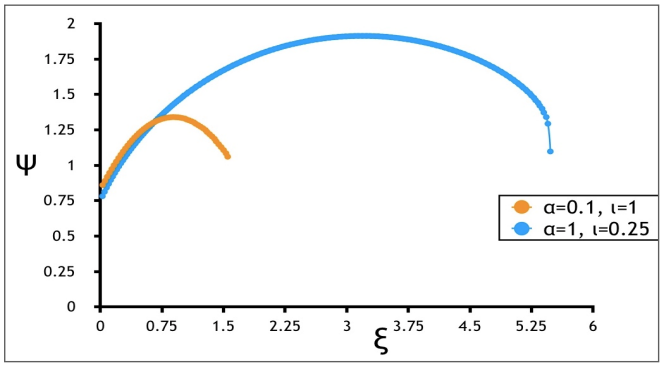

Figure 7. Electron velocity, ψ, as a function of position, ξ, within the sheath region of current bearing antiforce waves for wave speed values of α=0.1 and 1 and for current values of ι= 1 and 0.25 respectively.

Figure 7 represents dimensionless electron velocity, ψ, as a function of dimensionless position, ξ, within the sheath region of the wave. As wave speed decreases, sheath thickness increases considerably. For reference, the dimensionless sheath thickness ξ=1.5 represents an actual sheath thickness of $1.2x10^{-2}$m.

Figure 8 represents dimensionless electron temperature, θ, as a function of dimensionless position, ξ, within the sheath region of the wave. As wave speed decreases, electron gas temperature decreases considerably. For comparison with electron temperature reported by Jurenka and Barreto (1985), a dimensionless electron temperature value of θ = 6 represents an actual electron gas temperature of $3.48x10^6$ K. Our number represents the temperature at the core of the lightning return stroke.

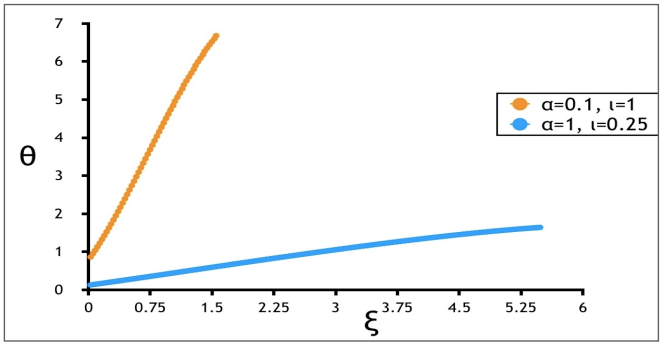

Figure 8. Electron temperature, θ, as a function of position, ξ, within the sheath region of current bearing antiforce waves for wave speed values of α=0.1 and 1 and for current values of ι= 1 and 0.25 respectively.

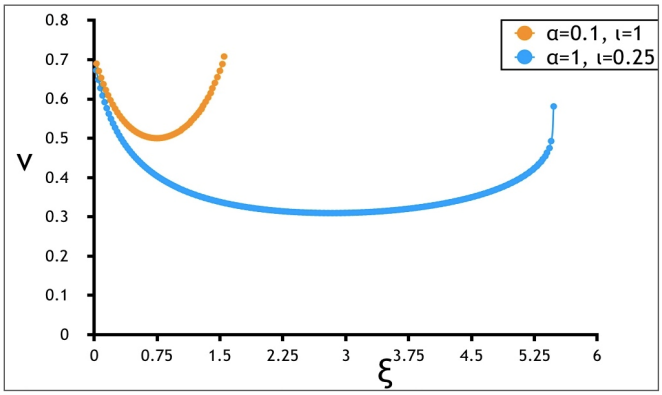

Figure 9. Electron number density, ν, as a function of position, ξ, within the sheath region of current bearing antiforce waves for wave speed values of α=0.1 and 1 and for current values of ι= 1 and 0.25 respectively.

Figure 9 represents electron number density, ν, as a function of dimensionless position, ξ, within the sheath region of the wave. The non-dimensional electron number density value of ν=0.7 represents an actual electron number density value of $7.7x10^{15}$ el./m^3, and

this almost agrees with the electron number density reported by Jurenka and Barreto (1985)

Figure 10 represents dimensionless ionization rate, μ, as a function of dimensionless position, ξ, within the sheath region of the wave. For the higher wave speed, ionization rate increases slightly, whereas for the lower wave speed, μ slowly decreases. For higher dimensionless current values and lower waves speeds, the integration of our set of electron fluid dynamical equations become difficult and very time consuming.

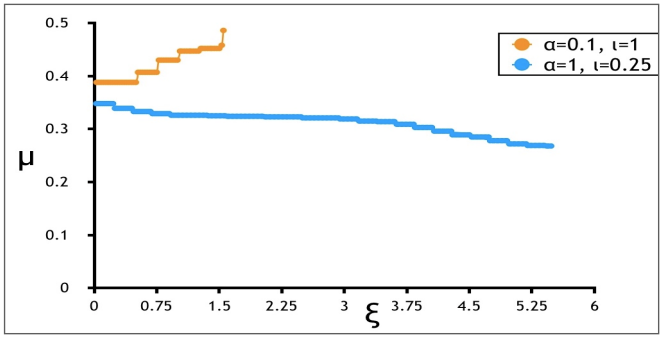

Figure 10. Ionization rate, μ, as a function of position, ξ, within the sheath region of current bearing antiforce waves for wave speed values of α=0.1 and 1 and for current values of ι= 1 and 0.25 respectively

Conclusion

We have been able to solve our set of electron fluid dynamical equations for a range of current values and also for a range of wave speed values. For the most part, the results of our integration agree with experimental data reported by others; however, we are able to integrate our set of equations for much lower wave speeds than reported experimentally.

For lightning return strokes, some investigators have suggested the existence of a relationship between the peak current values and wave speed values (Wagner (1963)). In other words, as the wave speed increases, the current that it can support increases as well. Some others (Willett *et. al* (1989)) disagree with the existence of such a relationship. We also confirm the existence of such a relationship.

Acknowledgments

We would like to express our gratitude for the financial support provided by the Arkansas Space Grant Consortium.

Literature Cited

Fowler RG, M Hemmati, RP Scott, and **S Parsenajadh.** 1984. Electric breakdown wave: exact numerical solutions. The Physics of Fluids 27(6):1521–1526.

Goto Y and **K Narita.** 1995. Electrical characteristics of winter lightning. Journal of Atmospheric and Terrestrial Physics 57:449-459.

Hemmati M. 1999. Electron shock waves: speed range for antiforce waves. Proceedings of the 22nd International Symposium on Shock Waves; 1999 July 18-23; Imperial College, London, UK. Pp. 2:995-1000.

Hemmati M, W Childs, H Shojaei, and **D Waters.** 2011. Antiforce current bearing waves. Proceedings of the 28th International Symposium on Shock Waves (ISSW28); 2011 July, England.

Idone VP, RE Orville, DM Mach, and **WD Rust.** 1987. The propagation speed of a positive lighting return stroke. Geophysical Research Letters 14(11):1150-1153.

Jurenka H and **E Barreto.** 1985. Electron waves in the electrical breakdown of gases, with application to the dart leader in lightning. Journal of Geophysical Research 90(D4):6219-6224.

Mach DM and WD Rust. 1992. Two dimensional velocity, optical risetime, and peak current estimates for natural positive lightning return strokes. Geophysical Research 98(D2):2635-2638.

Nakano M, M Nagatani, H Nakada, T Takeuti, and **Z Kawasaki.** 1987. Measurements of the velocity change of a lightning return stroke with height. Research Letters on Atmospheric Electricity 7:25-28.

Orville RE and GR Huffines. 1999. Lightning ground flash measurements over the contiguous United States. Monthly Weather Review 127:2693-2703.

Rakov VA. 2000. Positive and bipolar lightning discharges: a review. Bulletin of the American Meteorological Society 84(6):767-776.

Shelton GA and **RG Fowler.** 1968. Nature of fluid electron dynamical waves. The Physics of Fluids 11(4):740-746.

Wagner CF. 1963. Relation between the stroke current and velocity of return stroke. IEEE Transaction on Power Apparatus and Systems. 82:609-617.

Willett, JC, JC Bailey, VP Idone, A Eybert-Berared, and **L Barret.** 1989 Sub-Microsecond inter-comparison of radiation fields ad currents in triggered lightning return stroke based on the transmission-line. Journal of Geophysical Research 94:13275-13286.

https://scholarworks.uark.edu/jaas/vol72/iss1/8
DOI: https://doi.org/10.54119/jaas.2018.7222